Bioconjugate Chemistry

Article

pubs.acs.org/bc

Molecular Complex Composed of β-Cyclodextrin-Grafted Chitosan and pH-Sensitive Amphipathic Peptide for Enhancing Cellular Cholesterol Efflux under Acidic pH

Yuki Takechi-Haraya,[†,‡] Kento Tanaka,[†] Kohei Tsuji,[†] Yasuo Asami,[§] Hironori Izawa,[‡,∥] Akira Shigenaga,[†] Akira Otaka,[†] Hiroyuki Saito,[†] and Kohsaku Kawakami*[,‡]

[†]Institute of Health Biosciences, Graduate School of Pharmaceutical Sciences, The University of Tokushima, 1-78-1 Shoumachi, Tokushima 770-8505, Japan

[‡]International Center for Materials Nanoarchitectonics, National Institute for Materials Science, 1-1 Namiki, Tsukuba, Ibaraki 305-0044, Japan

[§]TA Instruments Japan, Inc., 5-2-4 Nishi-Gotanda, Shinagawa-ku, Tokyo, 141-0031 Japan

[∥]Department of Chemistry and Biotechnology, Graduate School of Engineering, Tottori University, 4-101 Koyama-Minami, Tottori 680-8552, Japan

Supporting Information

ABSTRACT: Excess of cholesterol in peripheral cells is known to lead to atherosclerosis. In this study, a molecular complex composed of β-cyclodextrin-grafted chitosan (BCC) and cellular cholesterol efflux enhancing peptide (CEEP), synthesized by modifying pH sensitive amphipathic GALA peptide, is introduced with the eventual aim of treating atherosclerosis. BCC has a markedly enhanced ability to induce cholesterol efflux from cell membranes compared to β-cyclodextrin, and the BCC-CEEP complex exhibited a 2-fold increase in cellular cholesterol efflux compared to BCC alone under weakly acidic conditions. Isothermal titration calorimetry and fluorescence spectroscopy measurements demonstrated that the random coil structure of CEEP at neutral pH converted to the α-helical structure at acidic pH, resulting in a three-order larger binding constant to BCC ($K = 3.7 \times 10^7$ at pH 5.5) compared to that at pH 7.4 ($K = 7.9 \times 10^4$). Such high-affinity binding of CEEP to BCC at acidic pH leads to the formation of 100-nm-sized aggregate with positive surface charge, which would efficiently interact with cell membranes and induce cholesterol efflux. Since the cholesterol efflux ability of HDL is thought to be impaired under acidic environments in advanced atherosclerotic lesions, the BCC-CEEP complex might serve as a novel nanomaterial for treating atherosclerosis.

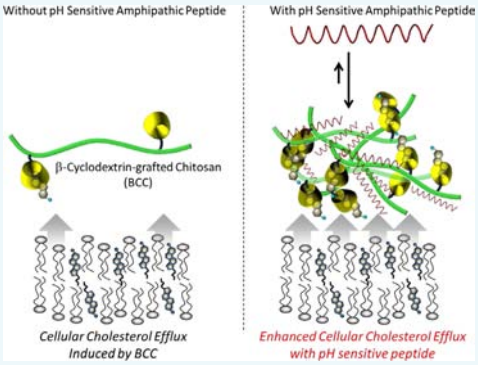

INTRODUCTION

Atherosclerosis is primarily the human disease related to cholesterol metabolism. Cellular cholesterol levels in mammal membranes are maintained within a narrow range by sophisticated and complex mechanisms.[1] One of the most established cholesterol regulations within cells is cholesterol efflux or reverse cholesterol transport mechanisms. The important extracellular acceptors for cholesterol are high-density lipoproteins (HDLs), whose major component is apolipoprotein A-I (apoA-I). So far, there is a well-known inverse correlation between HDL serum levels and the risk of atherogenesis leading to coronary heart disease.[2,3] The local concentration of HDL in the artery wall enhances cellular cholesterol efflux and protects against atherosclerosis in vivo.[4]

In advanced atherosclerotic lesions, it has been reported that the extracellular pH value decreases from 6.8 to 5.5 since the local concentration of lactate and proton is increased as in inflammatory conditions.[5,6] Such acidic pH increases the oxidation of lipoprotein by macrophages and decreases the expression of ABCA1 protein, which catalyzes the cholesterol efflux by apoA-I.[7−13] As a result, the development of the atherosclerotic plaque will be more progressive due to the decreased cholesterol efflux and inflammatory condition. Furthermore, at the inflammatory acidic pH microenvironment in advanced atherosclerotic lesions, the apoA-I in HDL is entrapped by proteoglycan binding and oxidized.[2,14] The cholesterol acceptor activity of HDL including that of oxidized apoA-I is low and the proteoglycan binding at acidic pH promotes misfolding, aggregation, and deposition as the amyloid-like structure of apoA-I, leading to atherogenesis.[15] Thus, without relying wholly on HDL/apoA-I-induced cholesterol efflux, the development of alternative therapeutic

Received: January 16, 2015
Revised: February 21, 2015
Published: February 23, 2015

DOI: 10.1021/acs.bioconjchem.5b00037
Bioconjugate Chem. 2015, 26, 572−581

strategies for atherosclerosis at acidic pH is of fundamental importance.[16]

Cyclodextrins (CyD), cyclic oligosaccharides consisting of glucopyranose units, are among the most potent compounds as vehicles to eliminate excess cellular cholesterols.[17] β-CyD (7 glucose units) has the highest affinity for encapsulating cholesterol compared to α (6 glucose units) and γ (8 glucose units) CyD.[18] In fact, β-CyD in the culture medium induces extensive release of cholesterol from a variety of cells in culture.[17,19] However, since the relatively high concentration of β-CyD (over 1 mM) is needed for the effective cellular cholesterol efflux, nonspecific binding of β-CyD to various types of biological constituent in serum, in particular, to erythrocyte, potentially becomes a problem with hemolysis.[17,20,21]

In our previous study, β-CyD-grafted chitosan (BCC) was synthesized for use as a multifunctional medical material, where BCC was found to form a complex with peptide effectively in relation to chitosan alone.[22] Chitosan is known to enhance membrane permeation/perturbation and absorption of lipids including cholesterol in intestine.[23−26] This study demonstrates the application of BCC as a potent cellular cholesterol efflux-inducing material. Also introduced is novel cellular cholesterol efflux enhancing peptide (CEEP) synthesized to introduce Tyr and Phe residues into pH-sensitive amphiphatic GALA peptide,[27,28] which exhibited high-affinity binding to BCC at pH 5.5 but low-affinity binding at pH 7.4. The acidic pH gives rise to 100-nm-sized BCC-CEEP aggregates which enhance cellular cholesterol efflux from HeLa cells. Compared to the experimental conditions without CEEP at pH 5.5, the cholesterol efflux induced by the BCC-CEEP complex exhibited a 2-fold increase. The mechanisms of the enhanced cellular cholesterol efflux are discussed by characterizing the formation of BCC-CEEP complex.

RESULTS AND DISCUSSION

BCC as a Cellular Cholesterol Efflux-Inducing Material. Uptake of cholesterol molecules by HDL acceptors involves partial exposure of their hydrophobic moiety to aqueous environment during the process,[29] for which the activation energy of cholesterol desorption was very high.[19] However, the activation energy for the CyD-mediated uptake of cholesterol becomes low compared to HDL,[19] suggesting that CyD molecules are substantially more efficient than HDL acceptors. In this study, we investigated the possibility of BCC to be a more potent cellular cholesterol efflux-inducing material than β-CyD. Figure 1 shows the comparison of cholesterol efflux from HeLa cells in the presence of BCC, BCC-20, or β-CyD. No significant cellular cholesterol efflux was observed at concentrations below 1 mM of β-CyD, which is consistent with previous reports.[17,30] In contrast, BCC and BCC-20 significantly induced the cholesterol efflux from HeLa cells at these concentrations, indicating that β-CyD grafted chitosan has a higher ability for cellular cholesterol efflux compared to β-CyD alone. The cellular cholesterol efflux induced by BCC was more effective compared to that of BCC-20, suggesting that the effective cholesterol efflux is attributed to local concentration of β-CyD. In fact, experimental and simulation research predicts the requirement of two β-CyDs to pull a cholesterol molecule into the hydrophobic cavity.[31−33] Thus, condensation of the β-CyD molecules near the cell membrane by connecting them by the polymer chain should be effective for the cholesterol efflux. Also, it is reported that membrane perturbation or packing

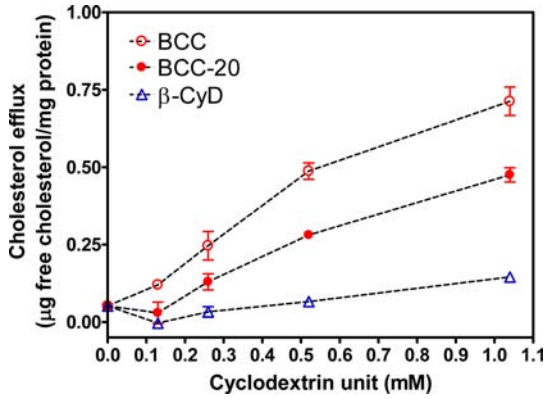

Figure 1. Comparison of cholesterol efflux from HeLa cells to BCC, BCC-20, or β-CyD as a function of CyD unit at pH 7.4. The experimental values are means ± SD (n = 6).

defects enhance the cholesterol uptake by β-CyD.[48] Chitosan backbone in BCC possibly induces the packing defect in the cell membrane, allowing cholesterol to desorb easily into the hydrophobic cavity of β-CyD. The insertion of chitosan into lipid membrane via both electrostatic, including hydrogen bonding, and hydrophobic interactions was reported previously.[23,26,34−37]

pH-Dependent Structure of CEEP. GALA is a well-known pH-responsive peptide which perturbs biological membranes at acidic pH by forming amphipathic α-helix.[28] At neutral pH, in contrast, the peptide does not interact with the membrane due to electrostatic repulsion of negative charges of deprotonated Glu residues.[38−41] In this study, we have developed CEEP by introducing 3 Tyr and 2 Phe residues into the GALA sequence without affecting the hydrophobicity and amphipathic helix character of the peptide (Figure 2A). The vector shows the hydrophobic moment ⟨μH⟩ as a measure of amphiphilicity of α-helix.[42] The ⟨μH⟩ of GALA and CEEP is 0.192 and 0.215, respectively. The mean hydrophobicity of the GALA and CEEP was calculated to be 0.471 and 0.484 by the Eisenberg scale.[43] Thus, our synthesized GALA derivative, CEEP, exhibits similar properties to GALA. The CD spectra of CEEP at various pH values (Figure 2B) demonstrated the formation of an α-helix structure of CEEP at acidic pH and a reversible structural change of CEEP between random coil and α-helix, in which the helix content of CEEP plateaus below pH 5.5 (Figure 2C). Thus, the net charge of CEEP is assumed to be 0 at pH 5.5 because of complete protonation of the Glu residues. We also analyzed the effects of electrostatic shielding on the structural change of CEEP by adding cations such as Na^+ and Ca^{2+} (Supporting Information Figure S2). The presence of 100 mM NaCl induced the α-helix structure of CEEP at pH 7.4, and further addition of $CaCl_2$ increased the α-helix content (Supporting Information Figure S2A,C). On the other hand, at pH 5.5, no structural change of CEEP was observed after the addition of Na^+ and/or Ca^{2+} ions (Supporting Information Figure S2B,C). Thus, CEEP is likely to alter its secondary structure from random coil to α-helix by decreasing the pH due to the protonation and/or electrostatic shielding of the Glu residues, and has the same structure below pH 5.5 due to complete protonation of Glu residues.

Formation of BCC-CEEP Complex and Its Function as a Cellular Cholesterol Efflux-Inducing Material. Interaction between materials and biological surfaces are significantly influenced by surface charges and the size of the

DOI: 10.1021/acs.bioconjchem.5b00037
Bioconjugate Chem. 2015, 26, 572−581

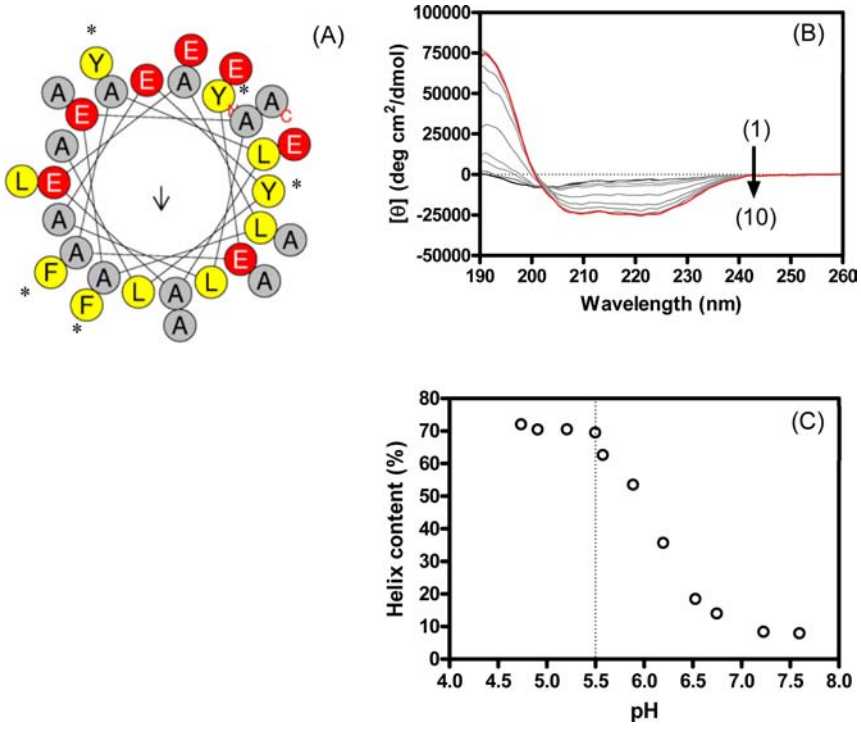

Figure 2. (A) Helical wheel diagram for amino acid sequence of CEEP arranged as an ideal α-helix (100° rotation per residue) seen down the long axis from the amino terminal end. The circular figure is rotated to orient the hydrophobic face toward the bottom of the page. The vector shows the hydrophobic moment $\langle\mu H\rangle$ as a measure of amphiphilicity of a helix. The $\langle\mu H\rangle$ of CEEP is 0.215. The mean hydrophobicity of the CEEP was calculated as 0.484 on the Eisenberg scale. (B) CD spectra of CEEP at various pH values: (1) 7.6, (2) 7.2, (3) 6.8, (4) 6.5, (5) 6.2, (6) 5.9, (7) 5.6, (8) 5.2, (9) 4.9, (10) 4.7. (C) α-Helical contents of CEEP calculated from $[\theta]_{222}$ as a function of solvent pH.

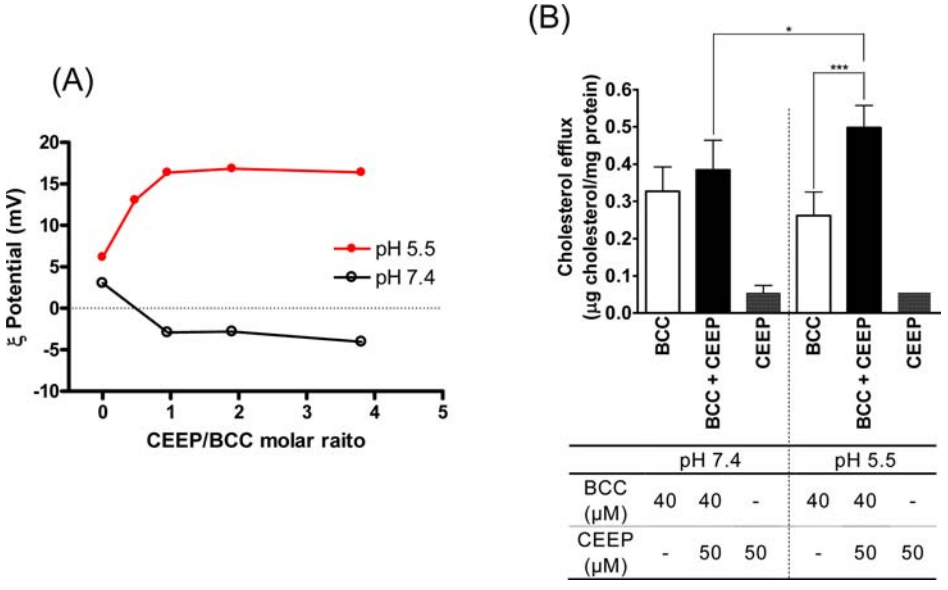

Figure 3. (A) ζ-Potential as a function of CEEP/BCC molar ratio at pH 5.5 or 7.4. The final concentration of BCC was fixed at 1 mg/mL. CEEP peptide was mixed with BCC so that the final concentrations of CEEP were 0.1−0.4 mg/mL. (B) Cholesterol efflux from HeLa cells to BCC in the absence or presence of CEEP peptide and efflux to CEEP were investigated at pH 5.5 and 7.4. Statistically significantly different: $^*P < 0.05$, $^{***}P < 0.001$. The experimental values were means ± SD ($n = 6$).

materials. Positively charged materials generally have strong affinity with negatively charged cellular membranes via electrostatic interaction. Figure 3A shows that the ζ potentials of BCC-CEEP nanoparticles under acidic and neutral pH conditions were ca. 17 and −3 mV, respectively, at a molar ratio of CEEP/BCC > 1. Below CEEP/BCC = 1, the decrease in the ζ-potential with increasing CEEP/BCC ratio at pH 7.4 can be explained by increase of the negative charges of CEEP due to the complex formation. The increase in the positive value of ζ potential at pH 5.5 may be explained by the increase in positive charge density of chitosan moiety due to the formation of "firm" BCC-CEEP aggregates. DLS measurements showed that the average size was approximately 125 and 19 nm at a molar

DOI: 10.1021/acs.bioconjchem.5b00037
Bioconjugate Chem. 2015, 26, 572−581

ratio of 3.8, at pH 5.5 and 7.4, respectively, indicating stronger interaction between CEEP and BCC at the acidic condition.

The effect of pH-sensitive CEEP on cellular cholesterol efflux by BCC was examined in HeLa cells at a molar ratio of CEEP/BCC = 1.25 (Figure 3B). Note that cholesterol efflux induced by the addition of CyD alone at the same concentration is almost negligible under both pH values, and chitosan does not have sufficient solubility to conduct this study. At pH 7.4, the cholesterol efflux in the presence of the BCC-CEEP mixture was identical to that of BCC. In contrast, the coexistence of CEEP significantly increased the cholesterol efflux induced by BCC at pH 5.5. CEEP does not induce cholesterol efflux at both pH 7.5 and 5.5. These observations indicated that CEEP has the potential to enhance the BCC-induced cellular cholesterol efflux solely at acidic pH. Regarding the mechanism of enhancement of cholesterol efflux ability of BCC at acidic pH, the pH-dependent membrane perturbation of CEEP was considered. Addition of CEEP to CF containing EPC/Chol vesicles caused CF leakage at pH 5.5, whereas this was not observed at pH 7.4 (Figure 4), suggesting pH-dependent action

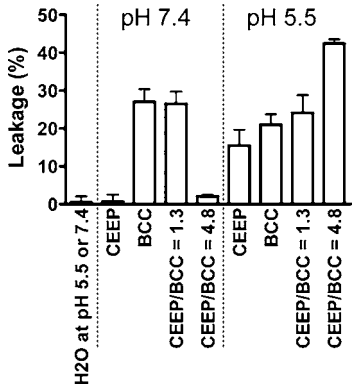

Figure 4. Leakage of CF from EPC/Chol vesicle at 3 min with the addition of various compounds is shown. The final concentrations of BCC and CEEP were 20 and 10 μg/mL, respectively. For the mixture of BCC and CEEP, the CEEP/BCC molar ratio was set to 1.3 (BCC = 20 μg/mL; CEEP = 3.4 ug/mL) or 4.8 (BCC = 20 μg/mL; CEEP = 13 μg/mL), respectively.

of CEEP on the lipid membrane. BCC induced the CF leakage as well, but the effect was not pH-dependent. Addition of CEEP to BCC enhanced the CF leakage at pH 5.5; however, it was suppressed at pH 7.5 in a concentration-dependent manner. Thus, CEEP is likely to cause membrane perturbation when it has the helix structure at pH 5.5, whereas it disturbs the activity of BCC by interacting with BCC and/or lipid membranes when it has the random-coil structure at pH 7.4. CEEP should also have the condensation effect of CyD moieties on the lipid membrane, because it has a strong interaction with BCC to form large aggregates at pH 5.5. This consideration is supported by the observation that cholesterol efflux is increased with increasing β-CyD density on the polymer chain (Figure 1).

Interaction between BCC and CEEP under Acidic pH. The binding enthalpy of BCC to CEEP was evaluated by injecting BCC into CEEP at a low BCC/CEEP molar ratio <1/200 at pH 5.5 (Supporting Information Figure S3A). Because of the large CEEP-to-BCC ratio, the injected BCC was likely to be completely bound to the peptide, and the heats of consecutive injections were almost constant (Supporting Information Figure S3B). The binding enthalpy at pH 5.5 exhibited large exothermic heat of −310.5 kJ/mol, suggesting that CEEP has a high affinity to BCC at acidic pH. The titration result at pH 5.5 is shown in Figure 5A, and the theoretical

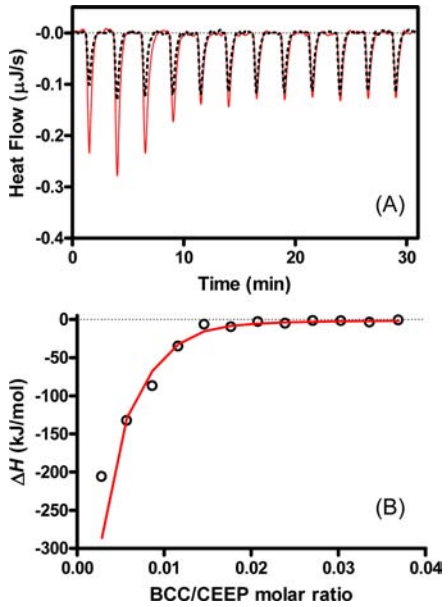

Figure 5. (A) ITC for BCC (6 μM) injection into CEEP peptide (30 μM) at pH 5.5. Each peak in the heat flowchart corresponds to the injection of 2.5 μL aliquots of BCC (solid line) at 25 °C. The heats of dilution were determined in control titrations by injecting BCC solution into pure buffer (dotted line). (B) Heats of reaction (integrated from the calorimetric trace) plotted as a function of the BCC/CEEP molar ratio. The heats of dilution were included in the final analysis. The solid line is the best fit to the experimental data using the complex formation model. Buffer: 50 mM acetate buffer containing 100 mM NaCl at pH 5.5. The calculated parameters are listed in Table 1.

fitting curve (Figure 5B) was derived from the integral heats as a function of BCC/CEEP molar ratio. The solid line in Figure 5B was the best least-squares fit to the data using eqs 1 and 2. The thermodynamic parameters were summarized in Table 1. The binding stoichiometry of peptide/BCC was ~110 at pH 5.5 and $K = 3.7 \times 10^7$ M^{-1}, demonstrating the strong interaction of CEEP with BCC at the acidic pH. The similar value of K, 4.4×10^6 M^{-1}, was obtained by fluorescence analysis (Table 1, Supporting Information Figure S4). Note that the binding of CEEP to BCC at pH 5.5 was driven not by entropy but by enthalpy (Table 1), suggesting that the BCC-CEEP interaction is dominated by electrostatic interaction. Interestingly, the value of binding stoichiometry at pH 5.5 corresponds approximately to the number of chitosan units in BCC structure. Because the negative charges of Glu residues in CEEP are likely to be protonated at pH 5.5, the electrostatic interaction between CEEP and BCC would arise from π electrons of Tyr and/or Phe residues with the protonated amine of chitosan units in BCC. This would lead to formation of the higher-order structure of peptide-BCC complex via inter-amphipathic helix−helix interaction or aromatic rings of Tyr and Phe residues.[44] The high value of stoichiometry at the acidic pH may also be explained by the electrostatic interaction between π electrons of Tyr and/or Phe residues with the protonated amine of chitosan units.

DOI: 10.1021/acs.bioconjchem.5b00037
Bioconjugate Chem. 2015, 26, 572−581

Table 1. Thermodynamic Parameters for the Interaction of CEEP Peptide with BCC

	binding stoichiometry (peptide/BCC)	K (M^{-1})	$\Delta G°$ (kJ/mol)	$\Delta H°$ (kJ/mol)	$T\Delta S°$ (kJ/mol)
pH 5.5[a]	111 ± 37	$(3.7 \pm 0.7) \times 10^7$	−42.2 ± 0.4	−310.5 ± 0.4	−268.3 ± 0.4
pH 5.5[b]	-	$(4.4 \pm 4.1) \times 10^6$	−34.1 ± 0.2	-	-
pH 7.4[b]	2 ± 1	$(7.9 \pm 6.1) \times 10^4$	−27.5 ± 1.9	-	-

[a]Determined by ITC measurement. Buffer: 50 mM sodium acetate buffer including 100 mM NaCl at pH 5.5. [b]Determined by fluorescence measurement. Buffer: 50 mM sodium acetate buffer including 100 mM NaCl at pH 5.5; 50 mM sodium phosphate buffer including 100 mM NaCl at pH 7.4.

Interaction between BCC and CEEP under Neutral pH. At pH 7.4, a reliable titration curve was not obtained by ITC due to the low exothermic heats (Supporting Information Figure S5), and the binding constant K was expected to be smaller than 10^5. Instead, change in the fluorescence spectra of CEEP upon addition of BCC was observed at pH 7.4 (Supporting Information Figure S6A). The binding constant K and binding stoichiometry at pH 7.4 were at least smaller by 2 orders of magnitude than those at pH 5.5 (Table 1, Supporting Information Figure S6C). Analysis using the Stern−Volmer plot[45] (Supporting Information Figure S7A) provided the K value of $(2.7 \pm 1.2) \times 10^4$ M^{-1}. Such low affinity binding of CEEP to BCC was not likely to induce the secondary structural change of the peptide (Supporting Information Figure S8). These results demonstrate that CEEP has pH-dependent binding affinity to BCC.

Since the chitosan backbone was assumed to play a dominant role in the complex formation of BCC with CEEP, the fluorescence spectra of CEEP was investigated with increasing concentration of chitosan (Supporting Information Figure S6B). The fluorescence quenching of CEEP was observed with increase in the chitosan concentration (Supporting Information Figure S6C). The binding constant and stoichiometry of CEEP to chitosan were almost similar to those for the BCC-CEEP system ($K = (8.2 \pm 3.1) \times 10^4$ M^{-1}, $n = 3 \pm 1$). At pH 7.4, electrostatic interaction between BCC and CEEP is thought to be small because the pK_a value of chitosan is ∼6.5.[24,46,47] The host−guest interaction of β-CyD units in BCC with Tyr and/or Phe residues of CEEP was not likely, because fluorescence spectra of CEEP did not change even with the addition of 50-fold excess molar of β-CyD (Supporting Information Figure S7B). Generally, the binding affinity of aromatic amino acids for hydrophobic cavity of β-CyD are as low as K = ∼10^2−10^3. Thus, the binding of CEEP to BCC appeared to be driven by nonspecific CH−π interaction between chitosan moiety in BCC and Tyr and Phe residues of CEEP, consistent with the fluorescence quenching of Tyr in the presence of BCC (Supporting Information Figure S6A). This assumption is also supported by the Near-UV CD spectra of CEEP in the presence of BCC (Supporting Information Figure S8, inset), demonstrating that the Tyr residues of CEEP interact with BCC since the amplitude of $[\theta]$ around 280 nm reflects the structural packing or order of the aromatic amino acids.[48−51]

Molecular Mechanism of the Strong Interaction of BCC with CEEP at Acidic pH. At acidic pH, Glu residues of CEEP are likely to be protonated. Thus, the intermolecular interaction is not due to ionic interaction between the Glu residues of CEEP and the positive charges of BCC. In addition, the amphiphatic α-helix formation of CEEP cannot fully explain the strong interaction between BCC and CEEP at pH 5.5, because CEEP did not have high affinity to BCC in the presence of 100 mM NaCl at pH7.4, where α-helix was formed (Table 1 and Supporting Information Figure S2C). Thus, the most likely mechanism of the high affinity of CEEP to BCC is the electrostatic interaction of the protonated amino group of the chitosan moiety in BCC with Tyr and/or Phe aromatic rings in CEEP.

To verify this assumption, we measured one-dimensional ^{1}H NMR spectra of BCC in the presence or absence of CEEP at pH 5.5 (Figure 6A). The spectra clearly showed that the ^{1}H NMR signal assigned to the C2-proton of the chitosan moiety in BCC is shifted toward a high magnetic field in the presence of CEEP, whereas it was not observed at pH 7.4 (Figure 6B). Accordingly, protonated amino group in BCC greatly contributes to the strong interaction with CEEP. CD spectra were also measured to investigate the structural change in CEEP bound to BCC (Figure 7). The far-UV CD spectrum of CEEP in the presence of BCC is almost identical to that in the presence of chitosan at pH 5.5 (Figure 7). The characteristic shape of the CD spectrum reflects the helix−helix interaction or aggregation of peptides. The ratio of the molar ellipticities at 222 and 208 nm ($[\theta]_{222}/[\theta]_{208}$) has been used as a criterion in several proteins to evaluate the presence of coiled-coil helices.

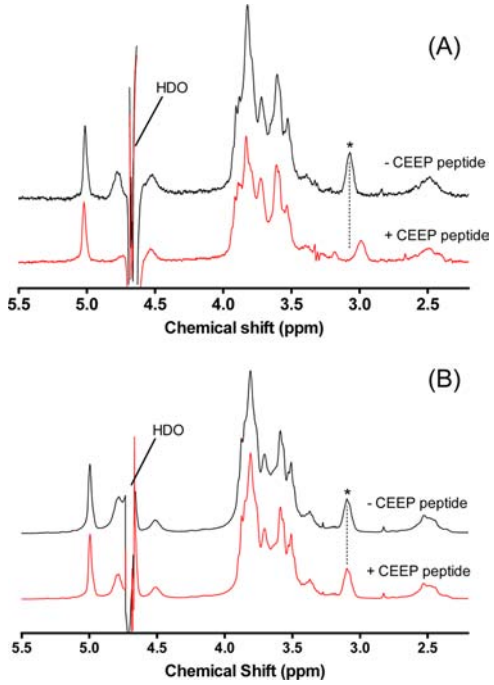

Figure 6. ^{1}H NMR spectra of BCC (-CEEP) or BCC-CEEP mixture (+ CEEP) at pH 5.5 (A) and 7.4 (B). The asterisks (*) in the spectra indicate the ^{1}H NMR signal assigned to C2 proton of chitosan moiety in BCC. The dotted lines are the auxiliary ones at the peak top of the proton signal in the absence of CEEP. The concentrations of CEEP and BCC were 0.3 and 1 mg/mL, respectively. The peak heights were normalized.

DOI: 10.1021/acs.bioconjchem.5b00037
Bioconjugate Chem. 2015, 26, 572−581

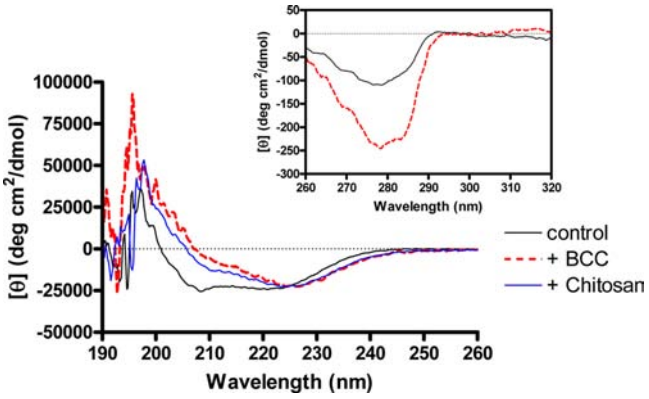

Figure 7. Effect of the presence of BCC or chitosan on the far-UV CD spectra of CEEP at pH 5.5. The concentrations of CEEP and BCC (or chitosan) were 50 and 300 μg/mL, respectively. The inset shows the near-UV CD spectra of CEEP in the presence or absence of BCC at pH 5.5. The concentrations of CEEP and BCC were 0.3 and 2 mg/mL, respectively.

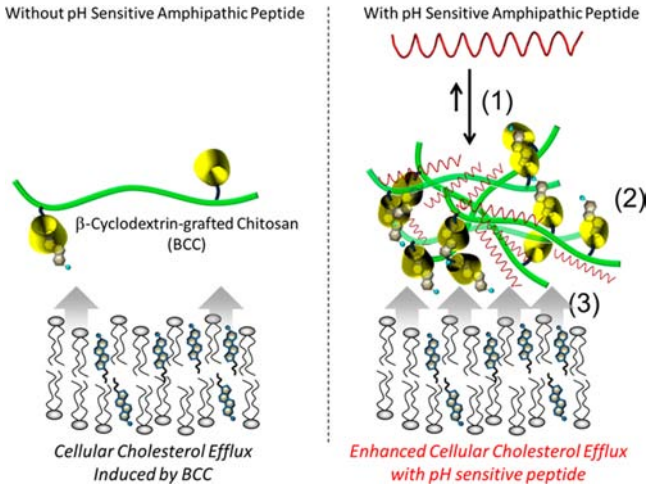

Figure 8. Proposed mechanisms of enhanced cellular cholesterol efflux induced by BCC with CEEP at acidic pH.

The ratio is <1 for a noninteracting α-helix while it is >1 for more than two-stranded coiled-coils.[52,53] The ratio of CEEP increased from 0.94 to 1.2 by the addition of BCC. This suggests the possibility of the formation of 100-nm-sized aggregate at the acidic pH via van der Waals interaction and/or hydrophobic interaction between Tyr and/or Phe residues in amphiphatic helices. The formation of the higher-order structure was supported by the result that an excess amount of BCC induces the fluorescence quenching of Tyr residues at pH 5.5 probably due to the light scattering by the aggregate or self-quenching by the formation of coiled-coil helices bound to BCC (Supporting Information Figure S9). Also, the interaction of Tyr residues with BCC was confirmed by near-UV CD spectra as a significant change in $[\theta]$ around 280 nm in the presence of BCC (Figure 7, inset). These results suggest a mechanism of the BCC-CEEP complex formation: CEEP strongly binds to BCC at acidic pH via the electrostatic cation$-\pi$ interaction between the protonated amino group of the chitosan moiety in BCC and the Tyr aromatic rings of the peptide, bridging BCC by the amphiphatic nature of α-helix of CEEP.

Mechanism of Enhanced Cellular Cholesterol Efflux Induced by BCC-CEEP Complex. The mechanism of the enhanced BCC-induced cellular cholesterol efflux by CEEP can be summarized as follows (Figure 8): (1) CEEP binds to BCC at acidic pH and induces aggregation of BCC via helix−helix interactions of the amphiphatic peptides. (2) The resultant BCC-CEEP aggregate has surface positive charges due to the protonation of amino group of chitosan moiety in BCC and form the condensed β-CyD surface in the aggregate. (3) The BCC-CEEP complex electrostatically interacts with cell membranes to induce perturbation more efficiently in the presence of amphipathic helix CEEP compared to BCC alone, and takes up cellular cholesterols into hydrophobic cavities of β-CyD units in BCC. Under neutral pH, this material is assumed to be inert due to absence of the positive charge and the amphipathic helix structure of CEEP. Thus, the BCC-CEEP complex can be expected as a building block of medical material to treat atherosclerosis.

CONCLUSIONS

We demonstrated the ability of β-cyclodextrin-grafted chitosan, BCC, as a more potent cellular cholesterol efflux-inducing material compared to β-CyD which is a representative agent to eliminate the cellular cholesterol. Moreover, we succeeded in adding pH-responsive function to BCC, by forming a complex with a cellular cholesterol efflux enhancing peptide, CEEP. It exhibits a random coil to α-helix transition in response to pH, and binds to BCC strongly only at acidic pH via the electrostatic cation$-\pi$ interaction to enhance the cholesterol efflux. The BCC-CEEP complex could be developed as a material for treating atherosclerosis because it has a strong ability to take up cholesterol from biological membranes under acidic condition.

MATERIALS AND METHODS

Materials. Chitosan (M_n: 22.6 kDa) was obtained from Yaizu Suisankagaku Industry (Shizuoka, Japan). The degree of deacetylation was determined to be 94.8% by elemental analysis. β-CyD were purchased from Nacalai Tesque (Kyoto, Japan). Mono(6-amino-6-deoxy)-β-cyclodextrin (β-CyD-NH_2) was prepared from β-CyD in accordance with a general method.[54] In addition, β-CyD−carboxylate was synthesized from β-CyD-NH_2 as described as our previous study.[22] The phospholipid, egg-yolk phosphatidylcholine (EPC, >95% pure), was purchased from NOF Corporation (Tokyo, Japan). The fatty acid compositions were as follows: 34−36% palmitic, 13% stearic, 29% oleic, 18−19% linolenic, and 4% arachidonic acid. Thus, the gel to liquid-crystalline phase transition temperatures of EPC are <0 °C and lipids are in the liquid crystalline phase under experimental conditions. 5-(and 6-)Carboxyfluorescein (CF) was purchased from Wako Pure Chemical Industries (Osaka, Japan). All other reagents were of the highest grade available and used without further purification.

β-CyD-Grafted Chitosan (BCC). The detailed description of synthesis, purification, and structure characterization of BCC has been reported by our previous study.[22] The structure of BCC is shown in Supporting Information Figure S1. The averaged molecular weight was determined from gel permeation chromatography, ^{1}H NMR, and the elemental analysis as 30 800. The β-CyD-content (molar fraction for the glucosamine unit of chitosan) was calculated from the peak area of

DOI: 10.1021/acs.bioconjchem.5b00037
Bioconjugate Chem. 2015, 26, 572−581

anomeric protons of chitosan and β-CyD to be 8.1%. To test the effect of local density of β-CyD in BCC on the cellular cholesterol efflux, another β-CyD-grafted chitosan polymer which had a covalently grafted β-CyD per 20 glucosamine units was synthesized (BCC-20).

Peptide Synthesis. A cellular cholesterol efflux enhancing peptide (CEEP), peptide sequence Ac-YEAALAEALAEA-LAEYLAEAFYEALEAFAA-$CONH_2$ modified from pH sensitive GALA peptide,[27,28] was designed and synthesized using Fmoc chemistry. The design of CEEP is based on our previous observation of the complex formation of BCC-insulin, in which tyrosine and phenylalanine residues in insulin are responsible for binding to BCC.[22] Purification of CEEP was carried out by reverse-phase HPLC using a Cosmosil 5C18-AR-II column (Nacalai Tesque, Kyoto, Japan). CEEP was eluted with a linear gradient of acetonitrile and water containing 0.1% trifluoroacetic acid and detected by UV at 220 nm. The purity of the eluted CEEP was confirmed to be >99% by HPLC and electrospray ionization-mass spectrometry.

Isothermal Titration Calorimetry (ITC). ITC measurements were carried out on a NANO ITC LV calorimeter (TA Instruments, New Castle, DE, USA). To avoid air bubbles, peptide and BCC solutions were degassed under vacuum for 10 min before use. CEEP peptide was placed in the 177 μL reaction cell, and a solution of BCC placed in a 50 μL titration syringe was injected into the peptide in cell. The injections were repeated automatically at 25 °C under 350 rpm stirring. Enthalpies of binding of CEEP peptide to BCC were corrected for heats of BCC dilution and dissociation; these values were determined by titrating BCC into buffer alone. The ITC data were analyzed using the program NanoAnalyze provided by TA Instruments. The ITC results were fitted by the theoretical curve using a *complex formation model*,[55−57] in which each BCC molecule acts as a ligand (L) and the BCC is assumed to have n equivalent and independent binding sites. This can be described according to

$$\frac{[L]_b}{[P]_t} = \frac{nK[L]}{1 + K[L]} \tag{1}$$

where $[L]$ and $[L]_b$ are the concentrations of free and bound BCC, respectively, $[P]_t$ is the total concentration of CEEP, and K is the binding constant. The parameter, n, was translated into $1/n$ meaning binding stoichiometry peptide/BCC. The concentration of bound BCC is expressed as $[L]_b = [L]_t - [L]$, where $[L]_t$ is the total concentration of injected BCC. The heat observed upon the injection is proportional to the amount of bound BCC

$$\delta Q_i = \Delta H^\circ \cdot \delta[L]_{b,i} \cdot V \tag{2}$$

where δQ_i is the heat released in the ith injection, $\delta[L]_{b,i}$ is the increase in the bound BCC concentration upon injection i, and V is the volume of the calorimeter cell. The Gibbs free energy ΔG° and entropy ΔS° for binding of BCC to CEEP were obtained by the following equations:

$$\Delta G^\circ = -RT \ln K \tag{3}$$

$$T\Delta S^\circ = \Delta H^\circ - \Delta G^\circ \tag{4}$$

where T is the absolute temperature.

Fluorescence Spectroscopy. All fluorescence measurements were carried out using a Jasco FP-6500 fluorescence spectrophotometer (JASCO Corporation, Tokyo, Japan) at 25 °C. The binding affinities of CEEP to BCC K (M^{-1}) analyzed by the fluorescence intensity of Tyr residues in the peptide. The excitation wavelength was 278 nm. CEEP solution (25 μg/mL) in the presence and absence of BCC were measured. BCC was added to the solution so that the final concentrations of the polysaccharide were 6−360 μg/mL. For the analysis of fluorescence spectra at pH 5.5, we employed a Benesi−Hildebrand type equation:[58]

$$\frac{1}{F - F_0} = \frac{1}{Ka[BCC]} + \frac{1}{a} \tag{5}$$

where F, F_0, and a are the fluorescence of peptide solution in the presence and absence of BCC and a constant, respectively. [BCC] is the molar concentration of BCC. For the interaction at pH 7.4, The binding constant, K, and the binding stoichiometry peptide/BCC, $1/n$, can be calculated from the following equation[59−61]

$$\log \frac{F_0 - F}{F} = n \log K - n \log\left(\frac{1}{[D_t] - (F_0 - F)[P_t]/F_0}\right) \tag{6}$$

where F_0 and F are the fluorescence intensities before and after the addition of BCC as a quencher, respectively. $[D_t]$ and $[P_t]$ are the total quencher concentration and the total CEEP concentration, respectively. Equation 6 is essentially based on the complex formation model and advantageous to get the binding stoichiometry.[59,62] Therefore, the calculated parameters from eq 6 are comparable to the parameters from ITC analysis. By the plot of $\log(F_0 - F)/F$ versus $\log(1/[D_t] - (F_0 - F)[P_t]/F_0)$, the number of binding sites n and binding constant K were obtained.

Circular Dichroism (CD) Spectroscopy. CD spectra were determined at 25 °C on a Jasco J-820 Spectropolarimeter (JASCO Corporation, Tokyo, Japan) with a path length of either 0.01 cm (for the far-UV region, 260−190 nm, secondary structure) or 1 cm (for the near-UV region, 320−260 nm, tertiary structure). Far-UV spectra were recorded at 0.2 nm intervals, 1 nm bandwidth, 50 nm/min, and 1 s response time. Near-UV spectra were recorded at 0.2 nm intervals, 1 nm bandwidth, 20 nm/min, and 4 s response time. The baseline corrected before converting to mean residue ellipticities. The peptide stock solution of 1 mg/mL in 10 mM sodium phosphate buffer pH 7.4 was diluted to 50 μg/mL or 300 μg/mL peptide for the far-UV or near-UV region, respectively, with 10 mM sodium phosphate buffer or 100 mM acetate buffer to adjust the pH value to 7.4 or 5.5. For the BCC-CEEP mixture, CEEP was incubated with BCC for 30 min prior to measurements. The spectrum was corrected by subtracting the buffer baseline or a blank sample containing an identical concentration of BCC. The α-helix content (%) of peptide was determined from mean residue ellipiticity, $[\theta]$, at 222 nm as described by Scholtz et al.:[63] α-helix content (%) = $([\theta]_{222} - [\theta]_{coil})/([\theta]_{helix} - [\theta]_{coil}) \times 100$; $[\theta]_{helix} = -40\,000 \times (1 - 2.5/n) + 100t$; $[\theta]_{coil} = 640 - 45t$, where $[\theta]_{222}$ is the measured mean residue ellipticity at 222 nm expressed in degree cm^2 $dmol^{-1}$, $[\theta]_{helix}$ and $[\theta]_{coil}$ are the mean residue ellipticities of the completely helical and coiled forms of the peptide (at 222 nm, expressed in degree cm^2 $dmol^{-1}$), respectively, n is the number of amino acid residues, and t is the temperature in °C. For determination of the pH-dependent reversibility of the helix−coil transition, the solutions of CEEP peptide were prepared in 10 mM sodium phosphate buffer and the pH was adjusted with 3 N HCl or 5 N NaOH to the appropriate value.

DOI: 10.1021/acs.bioconjchem.5b00037
Bioconjugate Chem. 2015, 26, 572−581

NMR Spectroscopy. Stock solution of CEEP was prepared by dissolving the peptide powder at a concentration of 0.6 mg/mL in 10 mM phosphate buffer D_2O solution (PBS). The pH or pD of the PBS was set to 7.0 with a glass electrode since the corrected D^+ ion concentration, as pD_{corr}, is according to the equation, $pD_{corr} = pD_{read} + 0.40$,[64] where pD_{read} is the value without correction for the glass electrode solvent isotope artifact. BCC of 2 mg powder was dissolved in 5% CH_3COOD/D_2O solution. Adding the equal volumes of PBS, or the prepared solution of CEEP to BCC solution, the final concentration of CEEP and BCC were fixed to 0.3 and 1 mg/mL of 600 μL in a 5 mm NMR tube. The pD of the sample solution was adjusted to 7.0 or 5.1 with 6 M $NaOH/D_2O$ solution. The ^1H NMR spectra were collected at 399.8 MHz using a JEOL ECS400 NMR spectrometer (JEOL, Tokyo, Japan) equipped with a superconducting magnet of 9.4 T. A high-sensitivity multinuclear probe (JEOL, NM-40TH5AT/FG2) was used. All spectra were collected at 303 K. Although D_2O was selected as a solvent, the DANTE presaturation pulse sequence was applied to avoid the signal overlapping of impurity light water (HDO) with the target ^1H NMR peak. The digital resolution was 0.5 Hz (0.001 ppm). Spectra were processed by the JEOL DELTA software. Chemical shifts were obtained by referring to the absorption frequency of the solvent deuteron monitored as the lock signal. For one-dimensional ^1H NMR measurement, free induction decays (FIDs) were accumulated 2048 times to optimize S/N ratio of the spectra.

Hydrodynamic Radius and ζ Potential Measurements. Dynamic light scattering (DLS) and electrophoretic light scattering (ELS) of BCC polymer solution/suspension in the addition of CEEP peptide were measured using a Beckman Coulter, Delsa NANO C (Beckman Coulter, Inc., Brea, CA, USA). The obtained DLS data were analyzed by the cumulant algorithm. ζ Potentials were calculated from the Henry equation: $\zeta = u4\pi\eta/\varepsilon$, where u is the electrophoretic mobility or velocity determined by ELS, η is the viscosity of the liquid, and ε is the dielectric constant.

Vesicle Preparation and Leakage Assay. The procedures for vesicle preparation and leakage assay are described previously.[65] Briefly, EPC/Chol at a molar ratio of 5/1 (38.5 mg/3.86 mg) was dissolved in chloroform in a round-bottomed flask and dried at 30 °C with a rotary evaporator to produce thin, homogeneous lipid film. To obtain a multilamellar vesicle suspension, the lipid film was dispersed by vigorous vortexing in 1 mL of 100 mM phosphate buffer (pH 7.0) containing ~50 mM carboxy-fluoresceine (CF), of which the pH was preadjusted to 7.0 using sodium hydroxide (pK_a value of CF is ~6.4). At this concentration, the fluorescence from CF was confirmed to be self-quenched completely. The resultant suspension was subjected to ten cycles of freeze−thawing and was then passed through a Mini-extruder equipped with two stacked 0.1 μm polycarbonate filters (Avanti, Alabaster, AL, Canada). The vesicle dispersion was diluted 500 000 times with phosphate buffer (pH 7.4) or acetate buffer (pH 5.5) containing the desired amount of BCC, GALA, or BCC-GALA mixture. Fluorescence intensity was measured at 520 nm using an excitation wavelength of 488 nm. The percent leakage of CF was determined using fluorescence intensity corresponding to 100% leakage obtained in the presence of 1 wt % of Triton X-100, as described in the previous study.[66]

Cell Culture and Cellular Cholesterol Efflux Assay. Cellular cholesterol efflux assay was performed as described previously.[67] Briefly, HeLa cells were grown in a humidified incubator (5% CO_2) at 37 °C in Dulbecco's modified Eagle's medium (DMEM) supplemented with 10% heat-inactivated fetal bovine serum (FBS). HeLa cells were subcultured in 24-well plates at a density of 1.2×10^5 cells in DMEM containing 10% FBS. After 24 h incubation, the cells were washed twice with PBS and incubated with β-CyD, BCC, BCC-20, CEEP, or BCC-CEEP mixture at pH 5.5 or 7.4 in DMEM containing 0.02% BSA for 4 h. The cholesterol content in the medium was determined by a fluorescence enzyme assay.[68] Note that microscopic observation revealed that no morphology changes were induced for HeLa cells by the additives. Also, the cell viability was confirmed by measuring the amounts of proteins derived from cells, which were 100 ± 10% for all the samples. These values were used as a reference for comparing cholesterol efflux from each cell (vertical axis of Figure 1 and Figure 3B). For the comparison between BCC, BCC-20, and β-CyD, the concentrations of the compounds were corrected by the β-CyD unit. The results were presented as the means ± SD ($n = 6$). Statistical analysis was performed by one-way ANOVA followed by the Dunnet comparison tests using *GraphPad Prism* v 4.0.

■ ASSOCIATED CONTENT

Supporting Information

Additional figures as described. This material is available free of charge via the Internet at http://pubs.acs.org.

■ AUTHOR INFORMATION

Corresponding Author

*E-mail: kawakami.kohsaku@nims.go.jp. Tel: 81-29-860-4424. Fax: 81-29-860-4708.

Notes

The authors declare no competing financial interest.

■ ACKNOWLEDGMENTS

This work was partly supported by the research program for development of intelligent Tokushima artificial exosome (iTEX) from The University of Tokushima, and World Premier International Research Center (WPI) Initiative on Materials Nanoarchitectonics, MEXT, Japan.

■ ABBREVIATIONS

apoA-I, apolipoprotein A-I; BCC, β-CyD-grafted chitosan; CD, circular dichroism; CEEP, cholesterol efflux enhancing peptide; CF, 5-(and 6-)carboxyfluorescein; CyD, cyclodextrins; HDL, high-density lipoprotein; ITC, isothermal titration calorimetry

■ REFERENCES

(1) Maxfield, F. R., and Tabas, I. (2005) Role of cholesterol and lipid organization in disease. *Nature 438*, 612−621.

(2) Birner-gruenberger, R., Schittmayer, M., Holzer, M., and Marsche, G. (2014) Understanding high-density lipoprotein function in disease: recent advances in proteomics unravel the complexity of its composition and biology. *Prog. Lipid Res. 56*, 36−46.

(3) Leman, L. J., Maryanoff, B. E., and Ghadiri, M. R. (2014) Molecules that mimic apolipoprotein A-I: potential agents for treating atherosclerosis. *J. Med. Chem. 57*, 2169−2196.

(4) Major, A., Dove, D., and Ishiguro, H. (2001) Increased cholesterol efflux in apolipoprotein AI (ApoAI)−producing macrophages as a mechanism for reduced atherosclerosis in ApoAI (−/−) mice. *Arterioscler. Thromb. Vasc. Biol. 21*, 1790−1795.

DOI: 10.1021/acs.bioconjchem.5b00037
Bioconjugate Chem. 2015, 26, 572−581

(5) Tabas, I. (2002) Consequences of cellular cholesterol accumulation: basic concepts and physiological implications. *J. Clin. Invest. 110*, 905−911.
(6) Nagha, M., John, R., Naguib, S., Said, M., Grasu, R., Madjid, M., Willerson, J. T., and Casscells, W. (2002) pH Heterogeneity of human and rabbit atherosclerotic plaques; a new insight into detection of vulnerable plaque. *Atherosclerosis 164*, 27−35.
(7) Morgan, J., and Leake, D. S. (1993) Acidic pH increases the oxidation of LDL by macrophages. *FEBS Lett. 333*, 275−279.
(8) Lamb, D. J., and Leake, D. S. (1994) Acidic pH enables caeruloplasmin to catalyse the modification of low-density lipoprotein. *FEBS Lett. 338*, 122−126.
(9) Lamb, D. J., and Leake, D. S. (1994) Iron released from transferrin at acidic pH can catalyse the oxidation of low density lipoprotein. *FEBS Lett. 352*, 15−18.
(10) Leake, D. S. (1997) Does an acidic pH explain why low density lipoprotein is oxidised in atherosclerotic lesions? *Atherosclerosis 129*, 149−157.
(11) Patterson, R. A., and Leake, D. S. (1998) Human serum, cysteine and histidine inhibit the oxidation of low density lipoprotein less at acidic pH. *FEBS Lett. 434*, 317−321.
(12) Sneck, M., Nguyen, S. D., Pihlajamaa, T., Yohannes, G., Riekkola, M. L., Milne, R., Kovanen, P. T., and Oörni, K. (2012) Conformational changes of apoB-100 in SMase-modified LDL mediate formation of large aggregates at acidic pH. *J. Lipid Res. 53*, 1832−1839.
(13) Nguyen, S. D., Öörni, K., Lee-Rueckert, M., Pihlajamaa, T., Metso, J., Jauhiainen, M., and Kovanen, P. T. (2012) Spontaneous remodeling of HDL particles at acidic ph enhances their capacity to induce cholesterol efflux from human macrophage foam cells. *J. Lipid Res. 53*, 2115−2125.
(14) Ramella, N. A., Rimoldi, O. J., Prieto, E. D., Schinella, G. R., Sanchez, S. A., Jaureguiberry, M. S., Vela, M. E., Ferreira, S. T., Tricerri, M. A., and Susana, A. (2011) Human apolipoprotein A-I-derived amyloid: its association with atherosclerosis. *PLoS One 6*, e22532.
(15) Huang, Y., DiDonato, J. a, Levison, B. S., Schmitt, D., Li, L., Wu, Y., Buffa, J., Kim, T., Gerstenecker, G. S., Gu, X., et al. (2014) An abundant dysfunctional apolipoprotein A1 in human atheroma. *Nat. Med. 20*, 193−203.
(16) Lee-Rueckert, M., Lappalainen, J., Leinonen, H., Pihlajamaa, T., Jauhiainen, M., and Kovanen, P. T. (2010) Acidic extracellular environments strongly impair ABCA1-mediated cholesterol efflux from human macrophage foam cells. *Arterioscler. Thromb. Vasc. Biol. 30*, 1766−1772.
(17) Kilsdonk, E. P. C., Yancey, P. G., Stoudt, G. W., Bangerter, F. W., Johnson, W. J., Phillips, M. C., and Rothblat, G. H. (1995) Cellular cholesterol efflux mediated by cyclodextrins. *J. Biol. Chem. 270*, 17250−17256.
(18) Schneider, H. J., Hacket, F., Rüdiger, V., and Ikeda, H. (1998) NMR studies of cyclodextrins and cyclodextrin complexes. *Chem. Rev. 98*, 1755−1786.
(19) Yancey, P. G., Rodrigueza, W. V., Kilsdonk, E. P. C., Stoudt, G. W., Johnson, W. J., Phillips, M. C., and Rothblat, G. H. (1996) Cellular cholesterol efflux mediated by cyclodextrins: demonstration of kinetic pools and mechanism of efflux. *J. Biol. Chem. 271*, 16026−16034.
(20) Ohtani, Y., Irie, T., Uekama, K., Fukunaga, K., and Pitha, J. (1989) Differential effects of α-, β- and γ-cycloddextrins on human erythrocytes. *Eur. J. Biochem. 186*, 17−22.
(21) Irie, T., and Uekama, K. (1999) Cyclodextrins in peptide and protein delivery. *Adv. Drug Delivery Rev. 36*, 101−123.
(22) Daimon, Y., Izawa, H., Kawakami, K., Żywicki, P., Sakai, H., Abe, M., Hill, J. P., and Ariga, K. (2014) Media-dependent morphology of supramolecular aggregates of β-cyclodextrin-grafted chitosan and insulin through multivalent interactions. *J. Mater. Chem. B 2*, 1802−1812.
(23) Fang, N., Chan, V., Mao, H., and Leong, K. W. (2001) Interactions of phospholipid bilayer with chitosan: effect of molecular weight and pH. *Biomacromolecules 2*, 1161−1168.
(24) Singla, a K., and Chawla, M. (2001) Chitosan: some pharmaceutical and biological aspects–an update. *J. Pharm. Pharmacol. 53*, 1047−1067.
(25) Xu, G., Huang, X., Qiu, L., Wu, J., and Hu, Y. (2007) Mechanism study of chitosan on lipid metabolism in hyperlipidemic rats. *Asia Pac. J. Clin. Nutr. 16*, 313−317.
(26) Wydro, P., Krajewska, B., and Ha, K. (2007) Chitosan as a lipid binder: a Langmuir monolayer study of chitosan-lipid interactions. *Biomacromolecules 8*, 2611−2617.
(27) Plank, C., Zauner, W., and Wagner, E. (1998) Application of membrane-active peptides for drug and gene delivery across cellular membranes. *Adv. Drug Delivery Rev. 34*, 21−35.
(28) Li, W., and Szoka, F. C., Jr. (2004) GALA: a designed synthetic pH-responsive amphipathic peptide with applications in drug and gene delivery. *Adv. Drug Delivery Rev. 56*, 967−985.
(29) Phillips, M. C. (2014) Molecular mechanisms of cellular cholesterol efflux. *J. Biol. Chem. 289*, 24020−24029.
(30) Atger, V. M., de la Llera Moya, M., Stoudt, G. W., Rodrigueza, W. V., Phillips, M. C., and Rothblat, G. H. (1997) Cyclodextrins as catalysts for the removal of cholesterol from macrophage foam cells. *J. Clin. Invest. 99*, 773−780.
(31) Breslow, R., and Zhang, B. (1996) Cholesterol recognition and binding by cyclodextrin dimers. *J. Am. Chem. Soc. 7863*, 8495−8496.
(32) Choi, Y., Yang, C., Kim, H., and Jung, S. (2001) Molecular modeling studies of the B-cyclodextrin in monomer and dimer form as hosts for the complexation of cholesterol. *J. Incl. Phenom. Macrocycl. Chem. 39*, 71−76.
(33) López, C. A., de Vries, A. H., and Marrink, S. J. (2011) Molecular mechanism of cyclodextrin mediated cholesterol extraction. *PLoS Comput. Biol. 7*, e1002020.
(34) Yang, F., Cui, X., and Yang, X. (2002) Interaction of low-molecular-weight chitosan with mimic membrane studied by electrochemical methods and surface plasmon resonance. *Biophys. Chem. 99*, 99−106.
(35) Rabea, E. I., Stevens, C. V., Smagghe, G., and Steurbaut, W. (2003) Chitosan as antimicrobial agent: applications and mode of action. *Biomacromolecules 4*, 1457−1465.
(36) Qi, L., Xu, Z., Jiang, X., Hu, C., and Zou, X. (2004) Preparation and antibacterial activity of chitosan nanoparticles. *Carbohydr. Res. 339*, 2693−2700.
(37) Pavinatto, F. J., Caseli, L., Pavinatto, A., Santos, D. S., Nobre, T. M., Zaniquelli, M. E. D., Silva, H. S., Miranda, P. B., and de Oliveira, O. N., Jr. (2007) Probing chitosan and phospholipid interactions using langmuir and langmuir-blodgett films as cell membrane models. *Langmuir 23*, 7666−7671.
(38) Parente, R. A., Nirs, S., and Szoka, F. C., Jr. (1988) pH-dependent fusion of phosphatidylcholine small vesicles. *J. Biol. Chem. 263*, 4724−4730.
(39) Parente, R. A., Nadasdi, L., Subbarao, N. K., and Szoka, F. C., Jr. (1990) Association of a pH-sensitive peptide with membrane vesicles: role of amino acid sequence. *Biochemistry 29*, 8713−8719.
(40) Parente, R. A., Nir, S., and Szoka, F. C., Jr. (1990) Mechanism of leakage of phospholipid vesicle contents induced by the peptide GALA. *Biochemistry 29*, 8720−8728.
(41) Nicol, F., Nir, S., and Szoka, F. C., Jr. (1996) Effect of cholesterol and charge on pore formation in bilayer vesicles by a pH-sensitive peptide. *Biophys. J. 71*, 3288−3301.
(42) Jones, M. K., Anantharamaiah, G. M., and Segrest, J. P. (1992) Computer programs to identify and classify amphipathic alpha helical domains. *J. Lipid Res. 33*, 287−296.
(43) Eisenberg, D., Weiss, R. M., and Terwilliger, T. C. (1984) The hydrophobic moment detects periodicity in protein hydrophobicity. *Proc. Natl. Acad. Sci. U. S. A. 81*, 140−144.
(44) Tatko, C. D., and Waters, M. L. (2002) Selective aromatic interactions in beta-hairpin peptides. *J. Am. Chem. Soc. 124*, 9372−9373.
(45) Keizer, J. (1983) Nonlinear fluorescence quenching and the origin of positive curvature in Stern-Volmer plots. *J. Am. Chem. Soc. 105*, 1494−1498.

DOI: 10.1021/acs.bioconjchem.5b00037
Bioconjugate Chem. 2015, 26, 572−581

(46) Henriksen, I., Vhgen, S. R., Sande, S. A., Smistad, G., and Karlsen, J. (1997) Interactions between liposomes and chitosan II: effect of selected parameters on aggregation and leakage. *Int. J. Pharm. 146*, 193−204.
(47) Mansouri, S., Cuie, Y., Winnik, F., Shi, Q., Lavigne, P., Benderdour, M., Beaumont, E., and Fernandes, J. C. (2006) Characterization of folate-chitosan-DNA nanoparticles for gene therapy. *Biomaterials 27*, 2060−2065.
(48) Chakrabartty, A., Kortemme, T., Padmanabhan, S., and Baldwin, R. L. (1993) Aromatic side-chain contribution to far-ultraviolet circular dichroism of. *Biochemistry 32*, 5560−5565.
(49) Kelly, S. M., Jess, T. J., and Price, N. C. (2005) How to study proteins by circular dichroism. *Biochim. Biophys. Acta 1751*, 119−139.
(50) Manning, M. C., and Woody, R. W. (1989) Theoretical study of the contribution of aromatic side chains to the circular dichroism of basic bovine pancreatic trypsin inhibitor. *Biochemistry 28*, 8609−8613.
(51) Sreerama, N., Manning, M. C., Powers, M. E., Zhang, J. X., Goldenberg, D. P., and Woody, R. W. (1999) Tyrosine, phenylalanine, and disulfide contributions to the circular dichroism of proteins: circular dichroism spectra of wild-type and mutant bovine pancreatic trypsin inhibitor. *Biochemistry 38*, 10814−10822.
(52) Zhou, N. E., Kay, C. M., and Hodgess, R. S. (1992) Synthetic model proteins. *J. Biol. Chem. 267*, 2664−2670.
(53) Choy, N., Raussens, V., and Narayanaswami, V. (2003) Inter-molecular coiled-coil formation in human apolipoprotein E C-terminal domain. *J. Mol. Biol. 334*, 527−539.
(54) Tang, W., Muderawan, I. W., Ong, T. T., and Ng, S. C. (2007) Facile synthesis of positively charged monosubstituted α- and γ-cyclodextrins for chiral resolution of anionic racemates. *Tetrahedron: Asymmetry 18*, 1548−1553.
(55) Gonçalves, E., Kitas, E., and Seelig, J. (2005) Binding of oligoarginine to membrane lipids and heparan sulfate: structural and thermodynamic characterization of a cell-penetrating peptide. *Biochemistry 44*, 2692−2702.
(56) Ziegler, A., and Seelig, J. (2007) High affinity of the cell-penetrating peptide HIV-1 Tat-PTD for DNA. *Biochemistry 46*, 8138−8145.
(57) Ziegler, A., and Seelig, J. (2008) Binding and clustering of glycosaminoglycans: a common property of mono- and multivalent cell-penetrating compounds. *Biophys. J. 94*, 2142−2149.
(58) Kuntz, I. D., Gasparro, F. P., Johnston, M. D., and Taylor, R. P. (1968) Molecular interactions and the Benesi-Hildebrand equation. *J. Am. Chem. Soc. 90*, 4778−4781.
(59) Bi, S., Song, D., Tian, Y., Zhou, X., Liu, Z., and Zhang, H. (2005) Molecular spectroscopic study on the interaction of tetracyclines with serum albumins. *Spectrochim. Acta, Part A: Mol. Biomol. Spectrosc. 61*, 629−636.
(60) Wang, Y. Q., Zhang, H. M., Zhang, G. C., Tao, W. H., and Tang, S. H. (2007) Interaction of the flavonoid hesperidin with bovine serum albumin: a fluorescence quenching study. *J. Lumin. 126*, 211−218.
(61) Ding, F., Zhao, G., Huang, J., Sun, Y., and Zhang, L. (2009) Fluorescence spectroscopic investigation of the interaction between chloramphenicol and lysozyme. *Eur. J. Med. Chem. 44*, 4083−4089.
(62) Gao, D., Tian, Y., Bi, S., Chen, Y., Yu, A., and Zhang, H. (2005) Studies on the interaction of colloidal gold and serum albumins by spectral methods. *Spectrochim. Acta, Part A: Mol. Biomol. Spectrosc. 62*, 1203−1208.
(63) Scholtz, J. M., Qian, H., York, E. J., Stewart, J. M., and Baldwin, R. L. (1991) Parameters of helix-coil transition theory for alanine-based peptides of varying chain lengths in water. *Biopolymers 31*, 1463−1470.
(64) Connelly, G. P., Bai, Y., Jeng, M. F., and Englander, S. W. (1993) Isotope effects in peptide group hydrogen exchange. *Proteins 17*, 87−92.
(65) Kawakami, K., Nishihara, Y., and Hirano, K. (1999) Determination of the entrapped volume of liposomes: dilution method. *Anal. Biochem. 269*, 139−142.
(66) Takechi, Y., Yoshii, H., Tanaka, M., Kawakami, T., Aimoto, S., and Saito, H. (2011) Physicochemical mechanism for the enhanced ability of lipid membrane penetration of polyarginine. *Langmuir 27*, 7099−7107.
(67) Nagao, K., Hata, M., Tanaka, K., Takechi, Y., Nguyen, D., Dhanasekaran, P., Lund-Katz, S., Phillips, M. C., and Saito, H. (2014) The roles of C-terminal helices of human apolipoprotein A-I in formation of high-density lipoprotein particles. *Biochim. Biophys. Acta 1841*, 80−87.
(68) Amundson, D. M., and Zhou, M. (1999) Fluorometric method for the enzymatic determination of cholesterol. *J. Biochem. Biophys. Methods 38*, 43−52.

DOI: 10.1021/acs.bioconjchem.5b00037
Bioconjugate Chem. 2015, 26, 572−581